LUND UNIVERSITY
FACULTY OF ENGINEERING (LTH)

Assessment of promoter regulation in *Pseudomonas putida* using GFP and flow cytometry

Master's Degree project in Applied Microbiology

Luka Cululejevic

Supervisors
Marie Gorwa-Grauslund
Fredrik Lund

Examiner
Magnus Carlquist

Table of contents

Abstract 3

1. Introduction 4

2. Materials & Methods 7

2.1. Strains and plasmids 7

2.2. Molecular biology procedures 8

2.3. Cultivation media 9

2.4. Transformation 10

2.5. Strain characterization 10

2.6. Analytical procedures 11

3. Results 12

3.1. Plasmid construction 12

3.2. Microplate-assay 13

3.3. Shake flask experiment – Promoter comparison on glucose 15

3.4. Shake flask experiment – media comparison with p14g reporter strain TMBFL010 18

4. Discussion 23

5. Conclusion 25

6. Future work 25

7. References 26

Appendix 1 28

Appendix 2 29

Appendix 3 30

Abstract

Lignin is found in all biomass and is an abundant natural source of aromatic compounds. It has the potential to serve as a renewable raw material for a variety of chemicals currently derived from fossil fuel sources such as muconic acid, an important platform chemical. Kraft lignin is a waste stream from the pulp and paper industry. Upon depolymerization of softwood-derived lignin, aromatic compounds such as guaiacol and vanillin are released and they can be further converted to muconic acid with the help of metabolically engineered *Pseudomonas putida* strain. To optimize the bioconversion pathway, it is important to be able to regulate gene expression using appropriate promoters. However, the lack of well-characterized promoter libraries on aromatic compounds in *P. putida* could pose limits on further engineering efforts.

As a means to increase available genetic engineering tools, this project aimed to characterize a few promoters in this species. Two strong promoters, p14c and p14g, were chosen from a synthetic promoter library along a single common inducible promoter - lacIq-Ptrc. The promoters were coupled to a green fluorescent protein (GFP) gene in a plasmid construct. These plasmids were later introduced into *P. putida* to be evaluated in a common minimal medium. The expression was evaluated mainly through flow cytometry, but also through a simpler method relying on optical density-adjusted fluorometry. Fluorescence was followed over time to catch the variability in expression in different growth stages.

The p14g promoter that displayed the highest fluorescence on glucose, was further evaluated in various media containing different combination of guaiacol and vanillin to study their potential effects on expression.

The presence of vanillin in the medium caused a decrease in fluorescence (11%) and growth (20%) after six hours of cultivation but an almost equal increase was observed after 24-hours. Guaiacol showed growth inhibitory effects at concentrations of 5 mM and higher through an increased lag-phase (2-4 hours) and halving of the final optical density (OD). Its presence, however, increased the GFP expression by 20-28%, depending on media composition and time point. Additionally, guaiacol caused an increased expression variance among the cell population, relative to other media.

Both fluorescence-determining methods showed the same trend in terms of relative fluorescence between cultures in exponential growth, although these differences were of different magnitude.

1. Introduction

The pulp and paper industry pretreats a large amount of biomass yearly through the so-called Kraft process but utilizes only the cellulose and hemi-cellulose fractions, leaving the Kraft-lignin stream as a by-product for combustion (Cao et al., 2018; Nguyen et al., 2021). This is because current biorefineries are not able to cost efficiently produce value added products from lignin streams due to the complex and heterogenous nature of this polymer (Beckham et al., 2016; Wenger et al., 2020). The deployment of microbial cell factories in a low molecular weight lignin environment has shown to be a promising approach at valorizing a variety of its compounds, without the excessive need for separation and purification (Abdelaziz et al., 2016; Cajnko et al., 2021). Alkaline depolymerization of soft-wood based Kraft lignin frees up a stream containing, among others, monoaromatic subunits of which guaiacol and vanillin are most abundant, in that specific order (Abdelaziz et al., 2018).

Pseudomonas putida is a gram-negative soil bacterium known for its versatile and robust metabolism and ability to survive in harsh environmental conditions (Chen & Wan, 2017; Lee et al., 2020). It can naturally catabolize the common lignin derived aromatic compounds such as *p*-coumarate, ferulate and vanillate through the β-ketoadipate pathway (Ravi et al., 2017). Depending on the starting substrate, it either goes through the protocatechuate (PCA) or catechol branch as seen in Figure 1. The bacterium's natural ability to catabolize these compounds together with the available genetic engineering tools makes this a promising platform strain for future biotechnological approaches for lignin valorization (Wackett, 2003; Weimer et al., 2020). Metabolic engineering of *P. putida* has enabled a two-step pathway conversion of guaiacol to muconate, a metabolic intermediate in the β-ketoadipate pathway (Almqvist et al., 2021). Muconic acid is a platform chemical most notably used in polymer production. It can notably be converted to adipic acid, caprolactam and terephthalic acid which are precursors for nylon-6,6, nylon-6 and polyethylene terephthalate (PET), respectively (Salvachúa et al., 2018). All the above-mentioned compounds have a global production in millions of metric ton ranges and are currently mostly derived from fossil fuel sources (GIA, 2021). From a life-cycle analysis perspective, production of muconic acid from Kraft lignin instead of fossil fuels could reduce greenhouse gas emissions (CO_2) up to 78% (Corona et al., 2018).

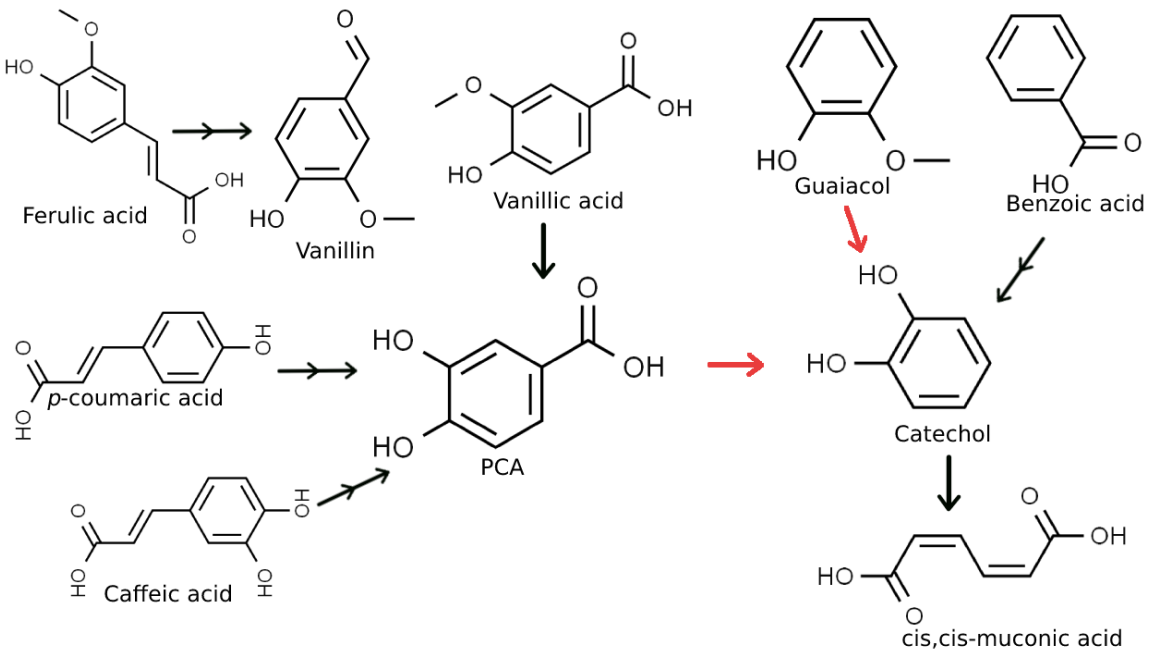

Figure 1. Simplified catabolic route from aromatic substrates to muconic acid in P. putida. *Red arrows indicate steps with introduced exogenous origin. Transformations shown with two arrows indicate multiple enzymatic steps.*

While recent studies have managed to demonstrate the conversion of several common lignin-based substrates to muconic acid at near theoretical yields, their titers and productivities remain a subject for improvement in order to be industrially relevant (Salvachúa et al., 2018). Tuning gene expression in genetically engineered pathways allows for flux optimizations which can significantly increase productivities, titers and yields (Hwang et al., 2018). A promoter is a DNA sequence to which the RNA polymerase binds in order to initiate transcription, see Figure 2. Depending on the sigma subunit's affinity toward the promoter, the transcription, and consequently the expression levels will vary. Exchanging a genes promoter is hence a great way to fine tune expression at the transcriptional level (Hartner et al., 2008). Some promoters, like the lac family, also have an upstream regulatory element repressing the promoter when an inducing compound is not present, such as isopropyl ß-D-1-thiogalactopyranoside (IPTG) in this case (Pelley, 2012). This is useful in scenarios where, for example, the product or metabolite is toxic and where it is more optimal to have separate growth and production phases (Ji et al., 2019).

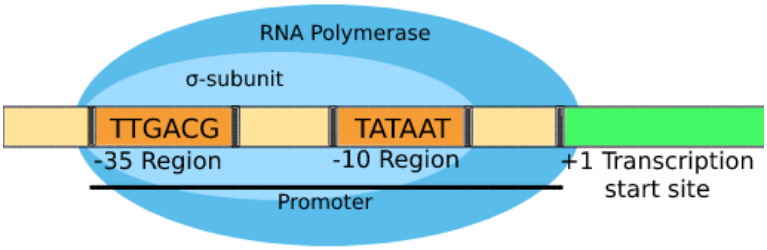

Figure 2. Illustration of a promoter (Adapted from LumeanLearning, 2022).

Currently, the amount of well characterized promoters and expression systems in *P. putida* remains low and for the most part relies on past knowledge from *Escherichia coli* libraries (Elmore et al., 2017). Some of the most used expression systems involve the xylS and lac regulated promoters while P_{T7}, P_{EM7} and P_{oprL} are some of the characterized constitutive promoters (Nikel & de Lorenzo, 2018). Although a promoter's total activity varies between the species, it has been shown that the relative performance of different promoters could be correlated in some cases (Zobel et al., 2015). This was, however, only demonstrated by a small sample size and gives only an expectation of a promoter's relative performance.

As a consequence, this study aims to increase the genetic toolbox available for precise engineering of *P. putida* through characterization of the strongest lacIq regulated promoter as well as two constitutive, synthetic promoters (Köbbing, 2020) on different carbon sources, including lignin-derived monomers. As a reporter protein for the promoters, green fluorescent protein (GFP) was employed in a plasmid-based set-up. Flow cytometry was chosen as the main method of determining GFP fluorescence in viable cells during different stages of growth.

A simpler, less time consuming but less accurate method of determining cellular GFP expression was also used. It consists in measuring total fluorescence and adjusting for the optical density (OD). The GFP expression does not offer a linear relation between fluorescence and growth in the lag- and stationary phase (Wirth & Nikel, 2021; Zobel et al., 2015). While no GFP expressing pattern is observed during the lag-phase, the GFP production continues after growth stops for some period before stopping, proposedly due to cell protein recycling (Köbbing, 2020). Both methods, however, have a linear fluorescence to OD relationship in the exponential growth phase and should hence be comparable (Wirth & Nikel, 2021; Zobel et al., 2015). As no known previous works have compared the two methods in *P. putida*, this method was also included in the present study.

2. Materials & Methods

2.1. Strains and plasmids

E. coli DH5α, used for subcloning of plasmids, and the wild type *P. putida* KT2440 were available from in house -80°C stocks. Plasmids p424 and p427M were ordered from the Standard European Vector Architecture (SEVA) (Madrid, Spain). All strains and plasmids, including those created in this work are listed in Table 1 and Table 2.

Table 1. List of plasmids used and constructed in this study.

Plasmid	**Relevant features**	**Reference**
p424	lacIq-Ptrc promoter; streptomycin resistance; RK2 Ori; T0 terminator	SEVA
p427M	msfGFP gene; streptomycin resistance; RK2 Ori; T0 terminator	SEVA
pFL008	p14g promoter; p424 backbone	This study
pFL0134	p14c promoter; p424 backbone	This study
pFL010	p14g; msfGFP gene; p424 backbone	This study
pFL014	p14c; msfGFP gene; p424 backbone	This study
pFL017	lacIq-Ptrc; msfGFP gene; p424 backbone	This study

Table 2. All strains used and constructed in this study.

Strain	**Relevant genotype**	**Reference**
E. coli DH5α	F^- endAI hsdRI7 (r^-_k, m_k^+) supE44 thi-l λ^- recAI gyrA96 relAI deoR Δ(lacZYA-argF)-U169 ϕ80dlacZΔM15	Seth G. et. al. 1990

P. putida KT2440	Control strain ("WT")	DSM 6125
E. coli pFL010	DH5α; pFL010 plasmid	This study
E. coli pFL014	DH5α; pFL014 plasmid	This study
E. coli pFL017	DH5α; pFL017 plasmid	This study
P. putida TMBFL010	KT2440; pFL010 plasmid	This study
P. putida TMBFL014	KT2440; pFL014 plasmid	This study
P. putida TMBFL015	KT2440; pFL017 plasmid	This study

2.2. Molecular biology procedures

All enzymes and reagents for the molecular biology procedures were supplied by Thermo Fisher Scientific (Waltham, US). Primers were ordered from Eurofins (Germany) and sequencing was done by the same company; primers and promoters are listed in Appendix 1. All procedures and calculations were done according to Thermo Fisher Scientific protocols and recommendations, respectively.

Plasmid p424 served as the vector for constructing the different promoter-msfGFP plasmids. A pair of primers with restriction site overhangs (5'-SacI, 3'-HindIII) were designed to PCR amplify the msfGFP gene found in plasmid p427M. The PCR product was confirmed through gel electrophoresis (0.8 w/v % agarose, 100V, 25min).

Plasmids pBG37 and pBG42 (SEVA) served as the source for the sequence of promoters p14c and p14g, respectively. For the two promoters, a set of 5'-phosphorylated primers were designed to bind right before the vector's promoter (lacIq-Ptrc) and at the multiple cloning site (MCS), running in opposite directions as illustrated in Figure 3. The primers had overhangs that carried a promoter's respective half at the 5' end. The PCR product was purified using Gene-Jet PCR purification kit and thereafter DpnI digested (FastDigest) to eliminate methylated template DNA. The blunt end purified PCR product was ligated using T4 DNA Ligase. The ligation product was lastly transformed into *E. coli* DH5α.

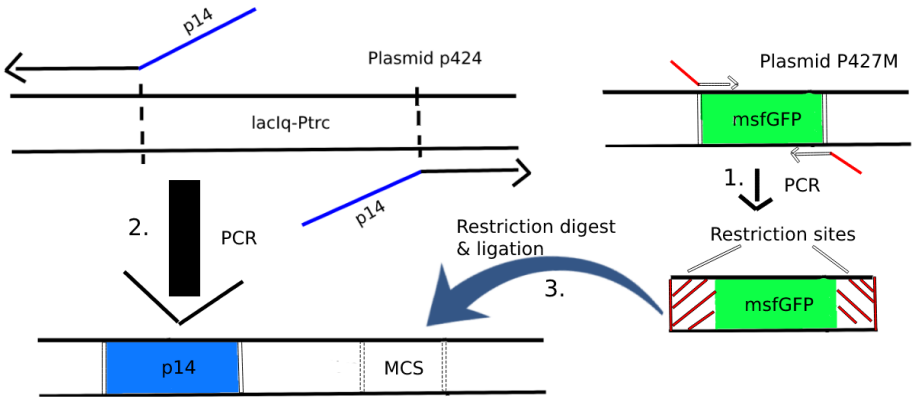

Figure 3. Workflow process of inserting the promoters (p14c, p14g) into the p424 plasmid and subsequently coupling a GFP gene to them. Step number two was skipped in making of the lacIq-Ptrc-GFP plasmid.

Colony PCR was performed on the transformed *E. coli* colonies using DreamTaq polymerase. Forward primers were unique to each promoter (p14c, p14g) while a p424 terminator primer served as a common reverse primer for colony PCR and Sanger sequencing of the final gene construct.

The p424 plasmids carrying promoters were digested at their MCS with SacI and HindIII, FastAP was added to dephosphorylate 5'-ends. The msfGFP amplicon was digested in the same manner, except FastAP was not included in the mix. Ligation was performed with a DNA insert to vector molar ratio of 3:1 using T4 DNA ligase. The plasmid constructs were introduced into *E. coli* DH5α and colony PCR was done to verify plasmid integrity before transforming *P. putida* KT2440.

2.3. Cultivation media

Lysogeny broth (LB) (10g/L tryptone, 5g/L yeast extract, 10g/L NaCl) was used for *E. coli* and *P. putida* cultivations during plasmid and strain construction. Plating out was done on LB agar plates (15 g/L agar). Media were supplemented with an antibiotic (100 µg/mL streptomycin or 50 µg/mL kanamycin) if the strain carried a selection marker. Incubation temperatures for *E. coli* and *P. putida* were 37°C and 30°C, respectively. Liquid cultures were shaken during incubation (flip-board or rotary shaker) and grown under aerobic conditions. Cell cultivation for plasmid construction and pre-cultures was done in 50 mL falcon tubes containing 5 mL medium. Glycerol stock solutions (25% w/v) of the constructed strains were made and stored in -80°C freezer.

Cultivations for promoter characterization were done in M9 minimal medium (12.8 g/L Na_2HPO_4, 3 g/L KH_2PO_4, 0.5 g/L NaCl, 1 g/L NH_4Cl, 2 mM $MgSO_4$, 0.1 mM $CaCl_2$, 5 mg/L EDTA disodium dihydrate, 2 mg/L $FeSO_4 \cdot 7\ H_2O$, 0.1 mg/L $ZnSO_4 \cdot 7\ H_2O$, 0.03 mg/L $MnCl_2 \cdot 4\ H_2O$, 0.3 mg/L H_3BO_3, 0.2 mg/L $CoCl_2 \cdot 6\ H_2O$, 0.01 mg/L $CuCl_2 \cdot 2\ H_2O$ or $CuSO_4 \cdot 5\ H_2O$,

0.02 mg/L $NiCl_2 \cdot 6\ H_2O$, 0.03 mg/L $Na_2MoO_4 \cdot 2\ H_2O$) supplemented with a single or mix of carbon sources (glucose, vanillin, guaiacol) at various concentrations. Induction of the lacIq-Ptrc system was done with 1 mM IPTG since it was reported as a saturating concentration for a lac regulated system in *P. putida* KT2440 (Sathesh-Prabu et al., 2021).

All pre-cultures were performed in M9 medium supplemented with 10 g/L glucose.

2.4. Transformation

Transformation of chemically competent *E. coli* DH5α cells followed a protocol by Inoue et al. (1990). The culture was plated on selective LB plates and incubated overnight at 37°C. Transformant colonies were verified with colony PCR and used to start a liquid culture the next day. Plasmid extraction was done using a Gene-Jet Plasmid miniprep kit (Thermo Fisher) following its protocol.

P. putida KT2440 transformation followed an in-house written protocol based on a protocol by Martínez-García and de Lorenzo (2012). An overnight preculture of *P. putida* KT2440 was used to inoculate a baffled 250 mL shake flask with 20 mL LB to an OD_{620} of 0.1. The cells were grown until OD_{620} of 0.8, they were then harvested by centrifugation (10 minutes, 3220g) and resuspended in 10 mL ice cold 300 mM sucrose solution. The cultures were washed with sucrose two additional times at a decreasing volume (1 mL - 500 µL) and then split into 100 µL aliquots. Excess aliquots were frozen in -80 °C freezer for future transformations. Plasmid (500 ng) was added to the aliquots and the mix was electroporated in 2mm wide electroporation cuvettes using Gene Pulser Xcell instrument (Biorad; 2.5 kV, 200 Ω, 25 µFD). Immediately after electroporation, 1 mL LB medium was added to the cuvette. The mix was transferred to an Eppendorf tube and incubated on a flip-board for 1.5 h at 30°C. Lastly, the cells were plated out overnight on selective LB agar plates and transformant colonies were verified with colony PCR before making a liquid culture for the glycerol stock.

2.5. Strain characterization

2.5.1. Micro-plate assay

An initial GFP expression experiment was done in a 96-well plate with two promoter strains (TMBFL010 & TMBFL014) and the WT strain (KT2440). Each strain was grown in M9 medium supplemented with one of seven carbon source mixes according to Table 3. The cells were cultivated for five hours on a micro-plate shaker, inside an incubator at 30 C°, before being analyzed. Technical duplicates were made and the starting OD_{620} for this experiment was approximately 0.4.

Table 3. *M9 media carbon compositions for the 96-well plate experiment.*

	1	2	3	4	5	6	7
Glucose	10 g/L	10 g/L	10 g/L	10 g/L	10 g/L	10 g/L	-
Vanillin	-	2.5 mM	5 mM	-	-	5 mM	5 mM
Guaiacol	-	-	-	5 mM	10 mM	10 mM	10 mM

2.5.2. Shake flask cultivations

Shake flask experiments were performed by first cultivating pre-cultures in M9 glucose medium overnight. The pre-cultures were used the following day to inoculate 250 mL baffled shake flasks containing 25 mL M9 medium with the chosen carbon source, to an OD_{620} 0.1. The lacIq-regulator was induced at the time of inoculation in the shake flask but not in the pre-cultures. The experiments were done in biological duplicates with samples taken at: 0 h, 2h, 4h, 6h and 24h. Analysis of the samples included OD_{620} measurements, fluorometry, flow cytometry.

In the first set of experiments, all promoter strains were evaluated in M9 glucose medium (10g/L). In the second set of experiments, *P. putida* TMBFL010 strain was evaluated in M9 medium supplemented with one of the following carbon sources; glucose 10 g/L (M9 glucose); glucose 10g/L and 5mM vanillin (M9 glucose+vanillin); glucose 10g/L and 10mM guaiacol (M9 glucose+guaiacol); 5mM vanillin and 10mM guaiacol (M9 guaiacol+vanillin). Sample analysis additionally included high performance liquid chromatography (HPLC) to monitor vanillin and guaiacol concentrations.

2.6. Analytical procedures

Upon sampling 1 mL from the shake flask, the sample tube was cooled for one minute on ice. A 400 μL aliquot was taken, cells spun down and the supernatant was frozen for later HPLC analysis. The rest was diluted with MQ water to $0.3>OD_{620}>0.03$ before being further analyzed.

2.6.1. Fluorometry

A 96-well plate was filled with 200 μL of the diluted samples and the OD_{620} was again determined by a microplate luminometer (Fluoroskan Ascent FL; 620 nm) followed by fluorometry in a microplate fluorometer (Fluoroskan Microplate Fluorometer; excitation 485 nm,

emission 538 nm). The fluorescence data was later divided with the OD-reading to get the OD-adjusted fluorescence.

2.6.2. Flow cytometry

A 200 μL aliquot (diluted with MQ water) was stained with 2 μL propidium iodine (PI) and incubated in dark for 15 minutes before being analyzed with a flow cytometer (BD Accuri C6 Plus). Forward scatter (FSC-H) threshold and number of events were set to 5000 and 25000, respectively. The fluorescence from GFP and PI were quantified in the FL1- (emission 533/30 nm) and FL3-channels (emission ≥ 670 nm), respectively. Raw data was exported as FCS files and processed using the software FlowJo. The raw data was processed by first excluding events with abnormal sizes and granularity (FSC-H and SSC-H) relative to the main cluster. The select events were further filtered by the exclusion of events high FL3 readings before finally determining the populations geometric mean fluorescence.

2.6.3. HPLC

HPLC samples were diluted to fit within the vanillin and guaiacol standard range (3mM – 0.05 mM). The instrument (Waters 2489) used a UV detector (281 nm) for detection. The mobile phase was a mix of 0.1% TFA and Millipore water (A), and acetonitrile (B). The C18 column was ran with a flow rate of 0.65 A and 0.35 B mL/min, respectively.

3. Results

First, the plasmids carrying the chosen promoter were constructed and introduced into *P. putida* (# 3.1). A micro-plate experiment was made to confirm the validity of the reporter strain and determine what aromatic compound concentrations influenced GFP expression (#3.2). The promoters' performance was then evaluated in a shake flask experiment (#3.3) and the strongest promoter was afterwards tested in different media, using chosen aromatic concentrations from the microplate experiment (#3.4).

3.1. Plasmid construction

In order to assess the promoter activity, the three promoters p14g, p14c and lacIq/ptrc were coupled to the monomeric superfolder green fluorescent protein (msfGFP) on a multicopy plasmid. This allowed the promoter activity to be quantified by measuring the fluorescence of the cells. The same ribosome binding site (RBS), terminator (T0), ori (RK2) and antibiotic resistance marker (SmR) were used in all three plasmids to reduce the number of factors that may affect the expression (see Figure 4). As seen in Table 4 the promoters' -35 and -10 motifs are identical, but the spacer region in between varies in sequence and GC content.

The three plasmids were introduced into *Pseudomonas putida* KT2440, resulting in the reporter strains TMBFL010 (p14g), TMBFL014 (p14c) and TMBFL015 (lacIq-Ptrc). The promoters' activity was evaluated primarily through flow cytometry and secondly through OD-adjusted fluorometry.

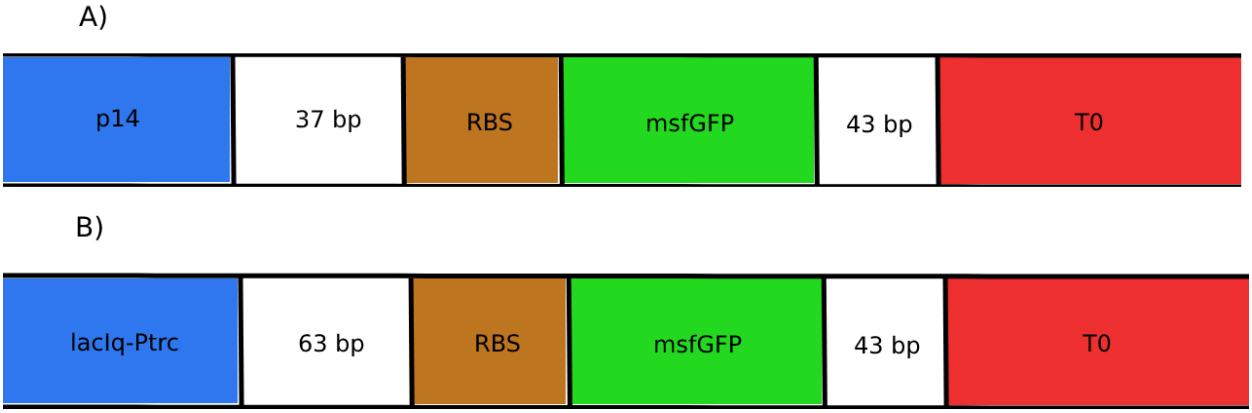

Figure 4. Representation of P. putida *TMBFL010 (A), TMBFL014(A) and TMBFL015 (B) strains' plasmid constructs. The ribosome binding site (brown), GFP gene (green), terminator (red) and backbone vector (p424) are identical in both constructs.*

Table 4. Promoter sequences and their -35 and -10 motifs colored in green and red, respectively. The spacing regions GC content, between the motifs, is also shown.

Promoter	Sequence	Spacer GC content (%)
p14g	GCCCATTGACAAGGCTCTCGCGGCCAGGTATAATTGCACGA	76
Ptrc	TTGACAATTAATCATCCGGCTCGTATAATG	47
p14c	GTGAATTGACATGTCAATTTTTATGTTGTATAATATAACTAC	24

3.2. Microplate-assay

In depolymerized Kraft lignin environment, *P. putida* is exposed to aromatic compounds, notably guaiacol and vanillin. It is hence interesting to know if relevant concentrations of those compounds can affect the activity of the investigated promoters and if there was a time-dependent correlation. Therefore, in order to verify the expression of GFP in the constructed strains, and to screen for relevant concentrations of vanillin and guaiacol that may affect the promoter activity, a 96 well-plate was first used to grow low volume cultures for five hours (to ensure exponential growth, see Appendix 2) and the fluorescence of the cultures was measured using fluorometry. Note that the lacIq-Ptrc strain is not included because it was not available yet at that time.

Media comparison

The results of the microplate fluorometry experiment are presented in Figure 5, with M9 glucose containing different levels and types of aromatic compounds and M9 glucose only as control. Fluorescence was detected in M9 glucose media in the 2 engineered strains but not in the control strain KT 2440, thereby validating the sensor functionality. The presence of 10mM guaiacol increased the fluorescence for the 2 tested promoters, whereas media with only vanillin or lower guaiacol level showed similar or decreased cellular fluorescence as compared to glucose. This was correlated with a limited increase in cell density in all media containing 10 mM guaiacol, see Figure 6. The presence of 2.5 mM guaiacol and the different vanillin concentrations did not have any effect on growth or fluorescence as compared to the control on glucose alone.

Promoter comparison

In this first experiment, the highest fluorescence per OD was observed with the p14g strain TMBFL010, followed by the p14c strain TMBFL014, for all conditions. But the p14c-dependent fluroescence was still much higher than for the negative control strain that showed low/no fluorescence in all media.

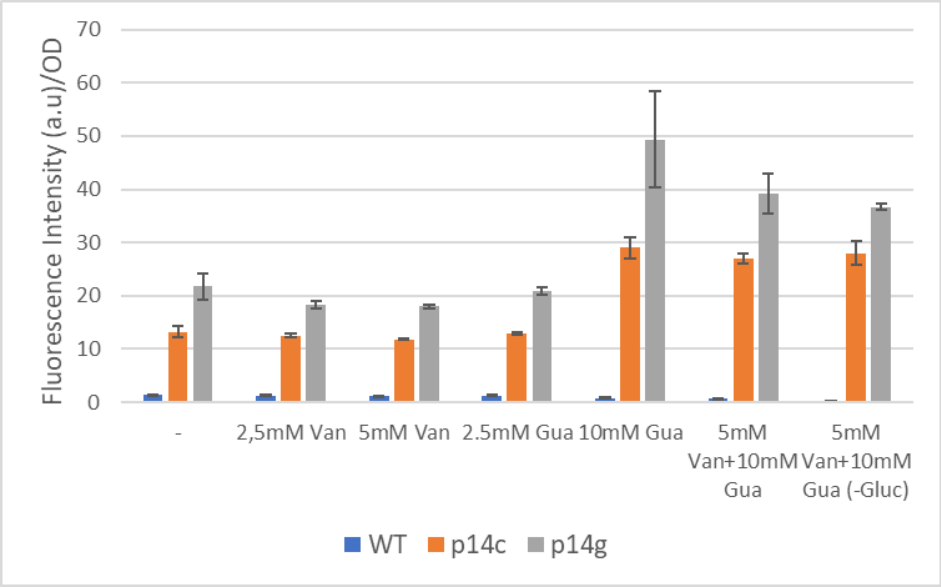

Figure 5. Microplate fluorometry data from P. putida *strains carrying a GFP gene behind different promoters and grown in M9 glucose media supplemented with compound(s) listed below the bars (Van = vanillin, Gua=guaiacol, Gluc=glucose). M9 glucose is used as the control medium, wild type is used as the negative control strain. Cells were grown for 5 hours with a starting* OD_{620} *0.4, error bars represent technical duplicates.*

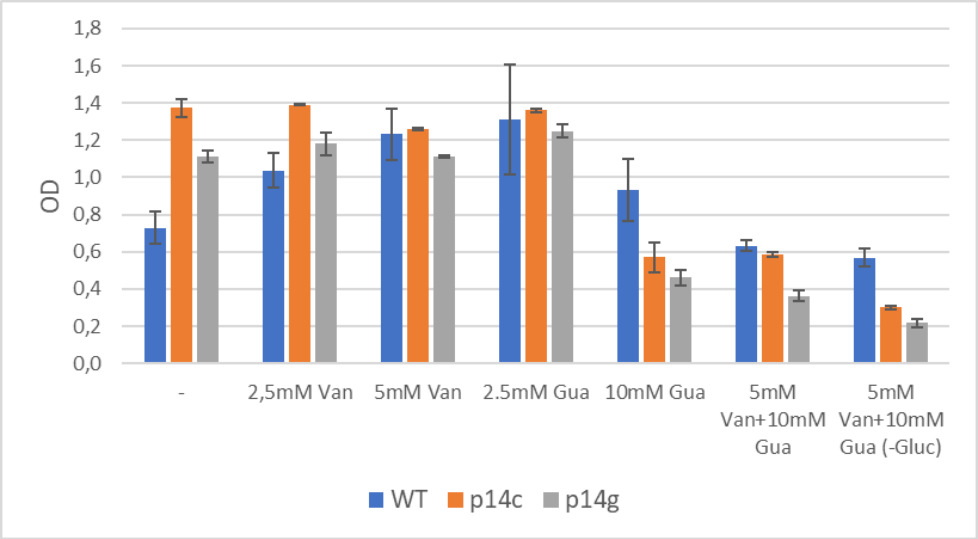

Figure 6. Microplate OD_{620} readings from P. putida *strains carrying a GFP gene behind different promoters and grown in M9 glucose media supplemented with compound(s) listed below the bars (Van = vanillin, Gua=guaiacol, Gluc=glucose). M9 glucose is used as the control medium while the wild type serves as the control strain for growth. Cells were grown for 5 hours with a starting OD_{620} 0.4, error bars represent technical duplicates.*

3.3. Shake flask experiment – Promoter comparison on glucose

Having confirmed the fluorescent activity of the promoters on both glucose and aromatic compounds through fluorometry, the relative performance of the promoter strains on glucose was further assessed in larger scale through a shake flask experiment using M9 glucose as medium. The fluorescence and growth were followed over one day in order to observe whether the expression changed over time. The fluorescence was determined through flow cytometry and OD-adjusted fluorometry for comparison of the two methods.

3.3.1. Flow cytometry

Processed flow cytometry data were visualized as histograms, as exemplified for time 6 and 24 hours in Figure 7. At both times, the peaks of p14g and laqIq-Ptrc displayed the highest fluorescence, followed by p14c, whereas the fluorescence remained low in the negative control. The p14g/p14c promoter peaks became slightly broader after 24 hours but kept their relative positions against each other. The inducible lacIq-Ptrc promoter showed a shift in the population distribution with a lower signal peak which represents approximately 20% of total events disappearing over time and with the higher signal peak becoming amplified.

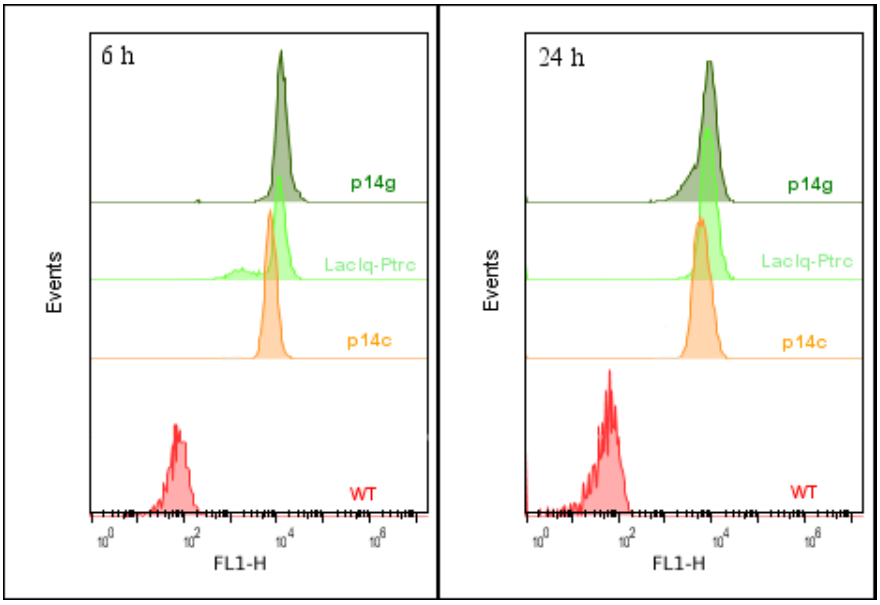

Figure 7. P. putida *promoter strains fluorescence histograms as recorded by the flow cytometer's FL1 detector channel. WT is the negative control strain. PI stained (non-viable) cells were filtered out using data from the FL3 detector channel. Left diagram is the six-hour sample, right diagram is the 24-hour sample.*

Geometric mean fluorescence over 24 hours is presented in Figure 8. Overall, the "constitutive promoters" p14g/p14c peaked at the time of inoculation and the GFP activity declined over time, with p14g losing 15% and p14c losing 27% after 6 hours of cultivation. In contrast, fluorescence of the IPTG-induced lacIq-Ptrc increased and stabilized after two hours and almost no loss in expression was observed over time. Still, p14g maintained the highest mean signal compared to lacIq-Ptrc by 43% and 19% in the 6h and 24h sample, respectively. But lacIq-Ptrc also had a stronger mean signal output than p14c from the 6 hour point (15% at 6h and 30% at 24h), although it was lower before the 6h data point.

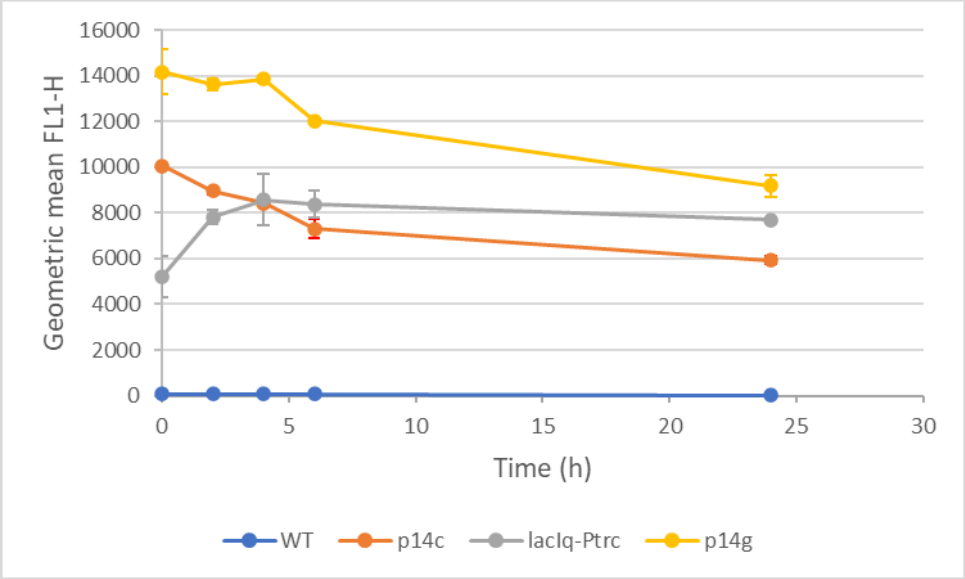

Figure 8. Geometric mean fluorescence of P. putida *strains carrying a GFP gene behind different promoters and grown in M9 glucose media. WT refers to the negative control strain KT2440. Fluorescence data was provided by flow cytometry using the FL1 detector, PI stained (non-viable) cells were filtered out using data from the FL3 detector. Experiments were performed in biological duplicate.*

3.3.2. Fluorometry

The OD_{620}-adjusted fluorescence of the different strains was also measured by fluorometry and is reported in Figure 9. Overall, p14g promoter remained the strongest promoter, followed by the IPTG-induced lacIq-Ptrc and p14c. However, using this method, there was an increase in fluorescence during the first two hours for the 3 sensors, followed by a decrease in the fourth hour and then lastly an upswing towards the end. The 24-hour OD-adjusted fluorescence ended up being higher than the starting ones for all strains (except the negative control strain); lacIq-Ptrc notably gained strength over p14g during that period. In numerical terms, p14g gave increased fluorescence against lacIq-Ptrc by 33% and 13% in the 6 and 24-hour samples, respectively. The lacIq-Ptrc strain has 10% and 44% stronger fluorescence in the respective samples than p14c. The relative fluorescence data of the two analytical methods' 6-hour samples was ordered in Table 5 for easier comparison.

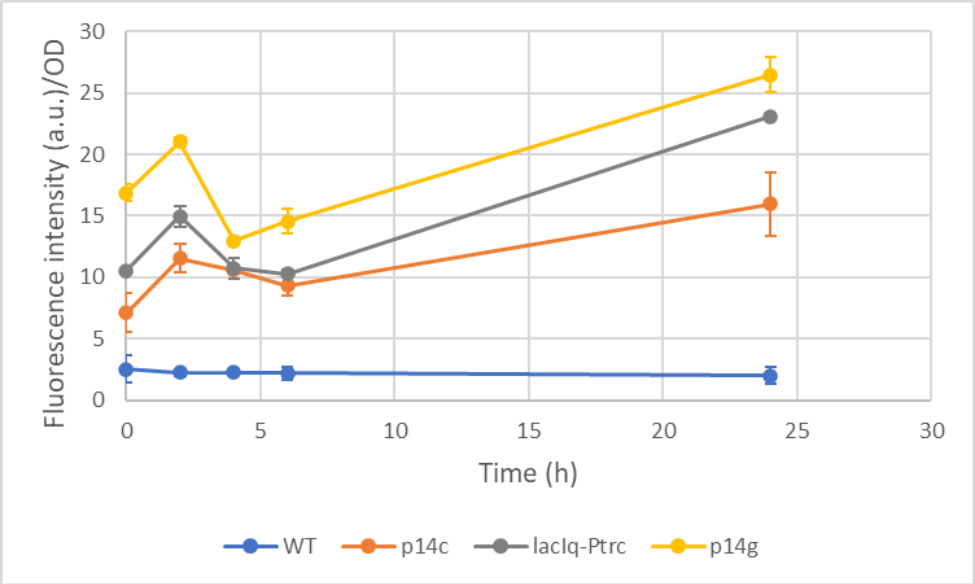

Figure 9. Fluorometry data of P. putida *promoter strains carrying a GFP gene behind different promoters and grown in M9 glucose media. Wild type represents the negative control strain. Experiment was performed in biological duplicates.*

Table 5. Relative fluorescence of P. putida *after 6 hours of cultivation using two analytical methods.*

Comparison pair	Flow cytometry increase	OD fluorometry increase
p14g/lacIq-Ptrc	43%	33%
p14g/p14c	64%	47%
lacIq-Ptrc/p14c	15%	10%

3.4. Shake flask experiment – media comparison with p14g reporter strain TMBFL010

The p14g strain TMBFL010 that displayed the highest fluorescence on M9 glucose (10 g/L) was further studied in three other M9 media: M9 glucose+ 5 mM vanillin, M9 glucose+10mM guaiacol and M9 5mM vanillin+10mM guaiacol, with M9 glucose as a control. TMBFL010 was grown in shake flasks under the four conditions for 24 hours and fluorescence was measured using flow cytometry and fluorometry every other hour for the first six hours. A final sample was taken after 24 hours.

3.4.1. Flow cytometry

The effect of media composition on GFP expression in strain TMBFL010, as measured by flow

cytometry, can be visualized in Figure 10 for the samples taken at 6 and 24 hours. The fluorescence distribution diagram at 6h showed that

- cells from M9 glucose+vanillin had a slightly weaker fluorescence than the other 3 conditions,
- cells in M9 glucose and M9 mix had similar fluorescence level
- cells in M9 glucose+guaiacol had a broader peak with asymmetrical sides compared to the other media.

-At 24h, cells from the M9 glucose and M9 glucose+guaiacol, displayed slightly broader peaks and stronger fluorescence than for the other two conditions.

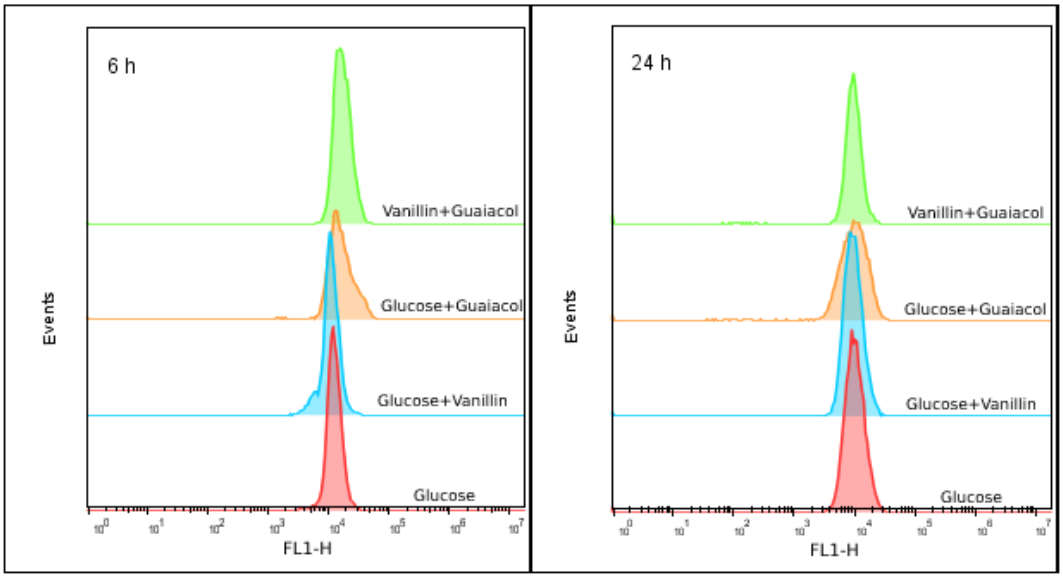

Figure 10. Fluorescence histograms of P. putida TMBFL010 grown in M9 media supplemented with different carbon sources, the left and right histograms represent the 6 h and 24 h samples of one replicate. Fluorescence data was acquired by flow cytometry using the FL1 detector, PI stained (non-viable) cells were filtered out with data from the FL3 detector.

Geometric mean fluorescence for the experimental timeframe is presented in Figure 11. The fluorescence increased during the first two hours in guaiacol containing media while remaining stable in the other media. After the first 2-4 hours, the fluorescence decreased continuously until 24-hours. In the 6-hour sample, cells incubated with guaiacol and the vanillin-guaiacol mix showed higher mean fluorescence than cells on M9 glucose by 20% and 28%, respectively. After 24 hours, M9 glucose+guaiacol had 24% increased fluorescence while M9 vanillin+guaiacol culture's fluorescence was only 5% lower relative to M9 glucose. Relative to M9 glucose, M9 glucose+vanillin had a 11% decrease at six hours followed by a 10% increase after 24 hours.

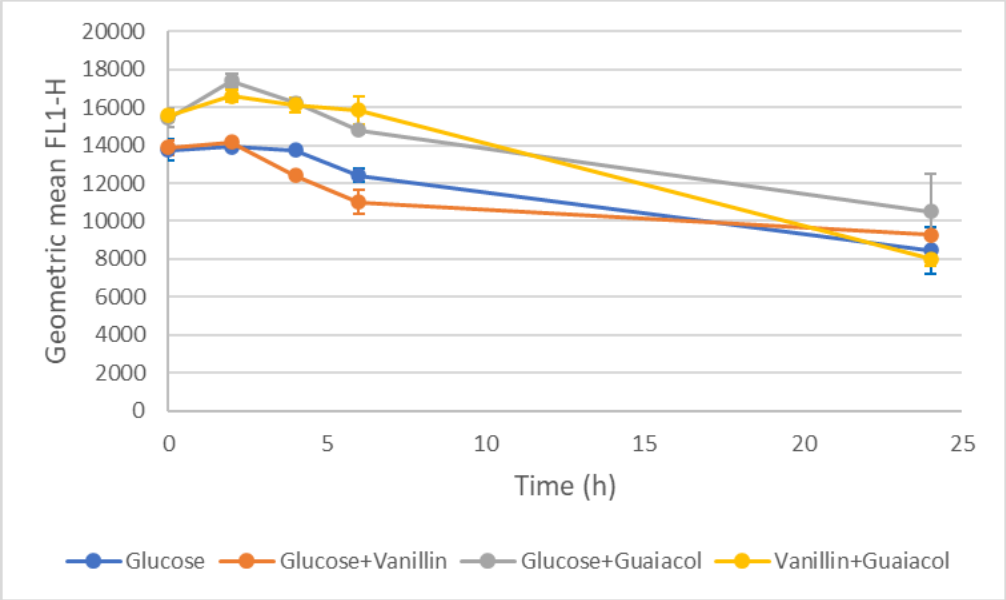

Figure 11. Geometric mean fluorescence of P. putida TMBFL010 in M9 media supplemented with different carbon sources. Fluorescence data was acquired by flow cytometry using the FL1 detector, PI stained (non-viable) cells were filtered out with data from the FL3 detector. Experiment was performed in biological duplicates.

3.4.2. Fluorometry

For the fluorescence measured by fluorometry the overall trend was similar in all media (Figure 12): an increase during the first two hours was followed by a decrease in the fourth hour and slight increase after 24-hours. Cells grown on glucose with guaiacol and a mix of guaiacol and vanillin exhibited higher fluorescence than on glucose alone (64% and 40% higher fluorescence in the 6-hour sample) while cells on glucose+vanillin had a slightly lower fluorescence than on glucose. The difference was smaller after 24 hours, and only cells on glucose+guaiacol had higher fluorescence than cells in other media.

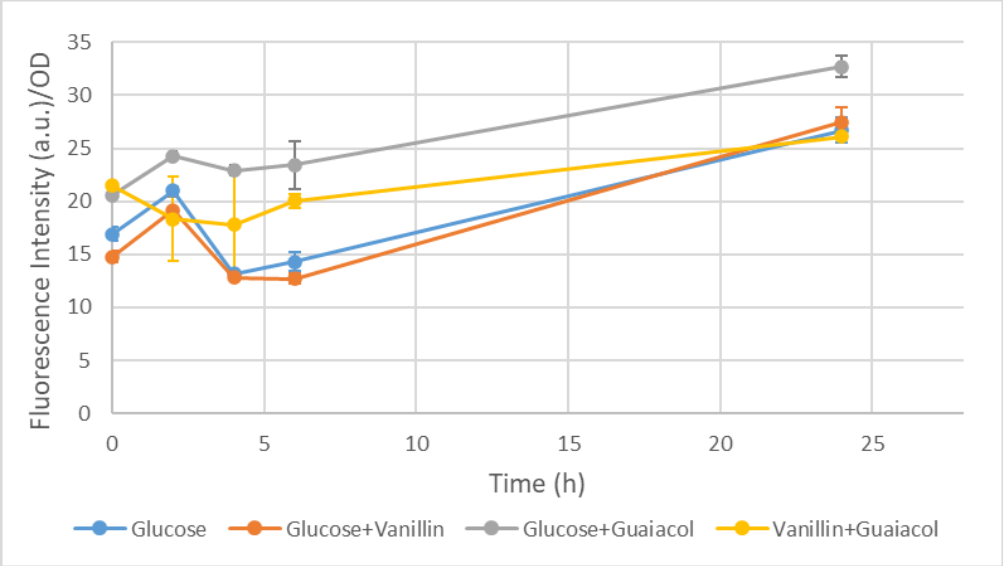

Figure 12. Fluorometry data of P. putida TMBFL010 grown in M9 media supplemented with different carbon sources. Experiment was performed in biological duplicates.

3.4.3. HPLC & Growth rate

In parallel to the GFP assessment, HPLC analysis was performed to follow the fate of guaiacol and vanillin over time. The results can be found in Figure 13. Guaiacol concentrations remained the same throughout the experiments while vanillin concentration decreased to zero. The consumption rate of vanillin was found to be slower in the presence of guaiacol (Figure 13). This confirmed the natural ability of the strain to use vanillin but not guaiacol (Ravi et al., 2018), and the inhibitory nature of guaiacol for *P. putida*.

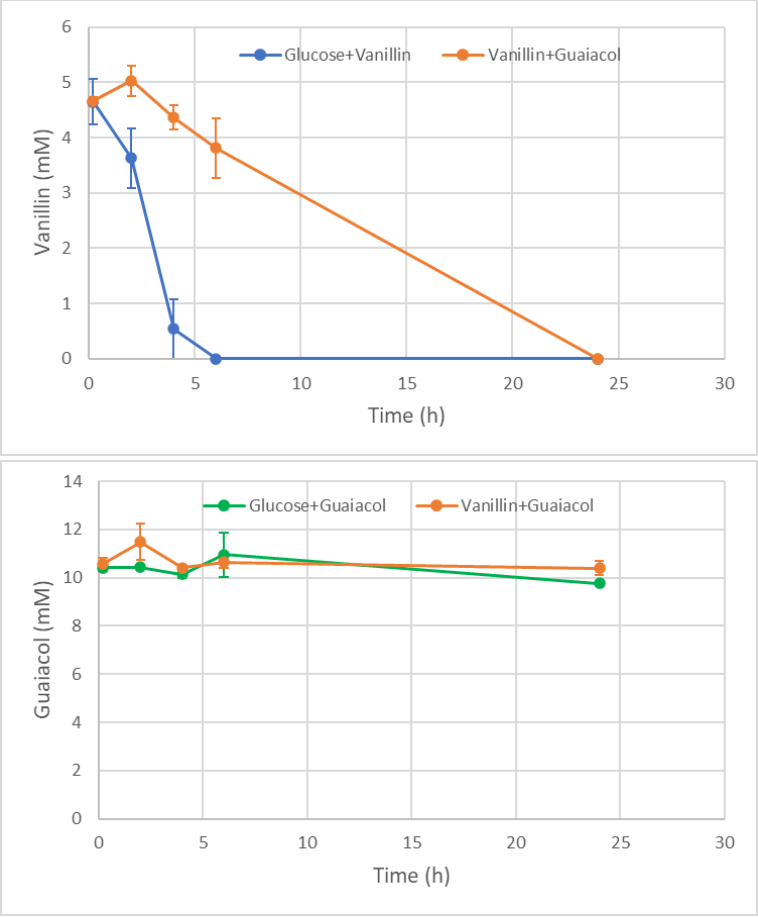

Figure 13. HPLC data from P. putida *TMBFL010 grown in M9 media supplemented with different carbon sources. Vanillin and guaiacol consumptions are shown in the upper- and lower diagram, respectively. Experiment was performed in biological duplicates.*

The effect of the aromatic compounds on the growth of TMBFL010 was also investigated by measuring the OD during the cultivations. The growth curves of the media comparison experiment are presented in Figure 14. Regarding lag-phase and growth rate, M9 glucose and M9 glucose+vanillin cultures follow each other closely, their final ODs being 3.8 and 4.5, respectively. Guaiacol containing media on the other hand, had a longer lag phase and also reached lower final ODs (2.3 and 0.3 on M9 glucose+guaiacol and M9 guaiacol+vanillin, respectively), confirming the inhibitory role of guaiacol on cell growth.

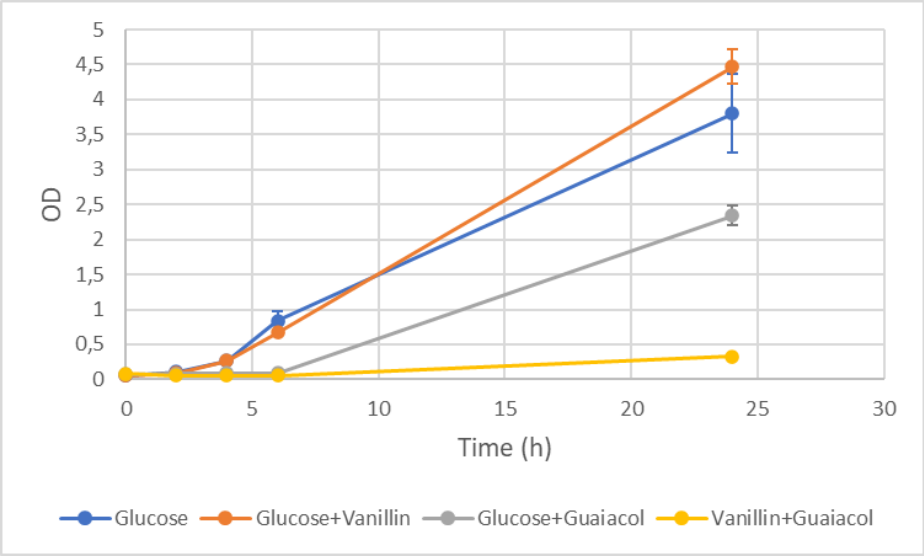

Figure 14. P. putida *TMBFL010 growth curves in M9 media supplemented with different carbon sources. OD measurement was performed with a microplate reader. Experiment was done in biological duplicates.*

4. Discussion

The objective of this study was to compare the activity of different promoters and their regulation over time and on different carbon sources. The synthetic promoters p14c and p14g, derived by randomizing the sequence surrounding the -10 and -35 (σ^{70}) promoter consensus regions (TATAAT and TTGACA), were chosen because they offered strong constitutive expression on *P. putida* (Zobel et al., 2015). The Ptrc promoter, a hybrid of the Ptrp (tryptophan) and Plac promoter that is commonly employed in lacIq-Ptrc regulated expression was also selected due to its strong activity upon induction (Camsund et al., 2014; Köbbing, 2020).

Glucose case

It was found that p14g promoter always displayed the highest GFP expression of the three tested promoters on glucose, with a relative expression to the p14c promoter that was in line with the original study (Zobel et al., 2015). The lacIq-Ptrc promoter had a comparable expression to p14c at 6 hours, although both were at significantly lower levels than p14g. Interestingly, this is the same order as the promoters' GC content in the spacer region, with p14g having the highest (76%) and p14c the lowest (24%). The same trend was observed by Zobel et al. (2015) upon comparing eight p14 promoters, suggesting that a high GC content in the spacer region might be beneficial to the promoter activity. An in-depth study suggested that a GC rich spacer content is less sensitive to DNA supercoiling (Klein et al., 2021). Another study, by Elmore et al. (2017), showed decreased promoter activity upon changing the -10 and -35 regions in *P. putida* KT2440, which might mean that the optimal σ^{70} motifs are shared with *E. coli*.

The inducible lacIq-Ptrc promoter was found to have a low-fluorescent subpopulation at 6 h (Figure 7) which shifted to the main population after 24 h, suggesting there were still non-induced cells at 6 h, which were induced at some point during the cultivation period. Since 1 mM IPTG was sufficient to induce a much higher cell density at 24 h and the molecule is otherwise stable in varying cultivation conditions, it is deemed that the observed 'lag' might be kinetics related (Politi et al., 2014). A slow induction can explain why the lacIq-Ptrc strain had a relatively stable fluorescence output while p14g and p14c strains experienced a 15% and 27% decrease in the exponential growth phase (6h), respectively. Protein dilution, which occurs during growth, is known to decrease cell GFP concentration and is correlated to the specific growth rate (Nordholt et al., 2017). Since the p14 promoter strain precultures had accumulated GFP before inoculation, more so than the non-induced lacIq-Ptrc strain, protein dilution caused by the reinitiated growth in the shake flask could be the reason behind the apparent decrease in fluorescence.

Aromatic case

The promoter p14g was also found to have the strongest expression when guaiacol was present in the media but slightly weaker than the control medium when vanillin was the sole aromatic compound. The fluorescence-distribution histogram suggests that guaiacol containing media causes a larger GFP expression variance among its cell population than other media. Equally strong expression was displayed by the strain during the first 6 hours when both aromatic compounds were present without any glucose supplement. Altogether this suggests that p14g promoter could be used in the presence of guaiacol and vanillin without any down-regulated activity.

In the studied strains, guaiacol could not be metabolized as the strains did not possess the needed genes. It was found that the compound inhibits cell growth at significantly lower concentrations (5 mM, see Appendix 2) than a guaiacol-converting strain derived from *P. putida* KT2440 (≥20 mM) (Almqvist et al., 2021). This could have affected the promoter's response. Therefore, additional tests of the promoter response to guaiacol should be performed using strains engineered for guaiacol utilization.

GFP assessment

Two methods were used to assess fluorescence: flow cytometry and OD-adjusted fluorometry. Overall, it was found that flow cytometry showed larger fluorescence differences among the strains and media than fluorometry although the strains were ranked in the same fluorescence order. Additionally, the fluorescence trend over-time was not correlated between the two methods as flow cytometry showed a continuous decrease while fluorometry had an increasing trend (excluding the drop between 2 h and 4 h).

In flow cytometry, fluorescence is measured on a single-cell level while fluorometry measures the bulk fluorescence of the culture and depends on optical density for relation to cell density. Inherently, fluorometry is less accurate as it catches noise from the media (media, excretions and cell debris) and depends on optical density as a proxy for the cell density. During cultivation, a buildup of GFP in the cell debris or change in cell morphology (larger cell size) could be the cause of increased OD-adjusted fluorescence over time. In contrast, the time between sampling and analysis is longer with flow cytometry and increases with sample number as parallel analysis is not possible, potentially allowing some metabolic activity to take place between sampling and analysis. Additionally, the data often needs further processing and the instrument is more expensive than a fluorometer (Hixson & Ward, 2022). Ultimately, fluorometry is not suitable for following GFP expression over time or accurately comparing GFP expression in *P. putida* strains. But it could be used as an initial, rapid screening method where accuracy is not important.

5. Conclusion

From the small promoter library constructed, p14g promoter proved to give the strongest expression during exponential growth. Hence, for genetic constructs in *P. putida* with strong constitutive expression, p14g should be preferred. Presence of 10 mM guaiacol in M9 glucose media was growth inhibitory but also stimulated higher cellular GFP expression on average. The bacteria could grow with strong GFP expression even when both aromatics were present and vanillin served as the sole carbon source, demonstrating a constitutive nature in the presence of those aromatics. The presence of 5 mM vanillin in M9 glucose media had a small negative effect on protein expression during exponential growth, but the opposite was observed in the stationary phase. The increased GFP expression in guaiacol media was possibly caused by the slower growth which allowed for a higher GFP accumulation level. Overall, OD adjusted fluorometry should not be used for accurate evaluation of GFP expression in *P. putida* live cell population because its readings, in terms of relative strain fluorescence as well as fluorescence over time were different to those of flow cytometry, but it could be a suitable initial screening method.

6. Future work

Extending the experiments to a biological triplicate could reduce the standard deviation so that more statistically significant conclusions can be drawn. Furthermore, sampling time points at 8 and 10 hours would be needed to study expression in exponential growth in media with 10 mM guaiacol. Further continuation to this work could include the introduction of the promoters behind guaiacol converting machinery genes and comparing how relatable the GFP production performance to guaiacol utilization. To get a better insight if the increased GFP expression under guaiacol’s presence is growth related, a similar experimental set-up could be done with a

guaiacol converting strain, which is not growth inhibited at 10 mM. Finally, the effect of plasmid copy number variation on expression levels could be further assessed.

7. References

Abdelaziz, O. Y., Brink, D. P., Prothmann, J., Ravi, K., Sun, M., García-Hidalgo, J., Sandahl, M., Hulteberg, C. P., Turner, C., Lidén, G., & Gorwa-Grauslund, M. F. (2016). Biological valorization of low molecular weight lignin. *Biotechnology Advances*, *34*(8), 1318-1346. https://doi.org/https://doi.org/10.1016/j.biotechadv.2016.10.001

Abdelaziz, O. Y., Li, K., Tunå, P., & Hulteberg, C. P. (2018). Continuous catalytic depolymerisation and conversion of industrial kraft lignin into low-molecular-weight aromatics. *Biomass Conversion and Biorefinery*, *8*(2), 455-470. https://doi.org/10.1007/s13399-017-0294-2

Almqvist, H., Veras, H., Li, K., Garcia Hidalgo, J., Hulteberg, C., Gorwa-Grauslund, M., Skorupa Parachin, N., & Carlquist, M. (2021). Muconic Acid Production Using Engineered Pseudomonas putida KT2440 and a Guaiacol-Rich Fraction Derived from Kraft Lignin. *ACS Sustainable Chemistry & Engineering*, *9*(24), 8097-8106. https://doi.org/10.1021/acssuschemeng.1c00933

Beckham, G. T., Johnson, C. W., Karp, E. M., Salvachúa, D., & Vardon, D. R. (2016). Opportunities and challenges in biological lignin valorization. *Current Opinion in Biotechnology*, *42*, 40-53. https://doi.org/https://doi.org/10.1016/j.copbio.2016.02.030

Cajnko, M. M., Oblak, J., Grilc, M., & Likozar, B. (2021). Enzymatic bioconversion process of lignin: mechanisms, reactions and kinetics. *Bioresource Technology*, *340*, 125655. https://doi.org/https://doi.org/10.1016/j.biortech.2021.125655

Camsund, D., Heidorn, T., & Lindblad, P. (2014). Design and analysis of LacI-repressed promoters and DNA-looping in a cyanobacterium. *J Biol Eng*, *8*(1), 4. https://doi.org/10.1186/1754-1611-8-4

Cao, L., Yu, I. K. M., Liu, Y., Ruan, X., Tsang, D. C. W., Hunt, A. J., Ok, Y. S., Song, H., & Zhang, S. (2018). Lignin valorization for the production of renewable chemicals: State-of-the-art review and future prospects. *Bioresource Technology*, *269*, 465-475. https://doi.org/https://doi.org/10.1016/j.biortech.2018.08.065

Chen, Z., & Wan, C. (2017). Biological valorization strategies for converting lignin into fuels and chemicals. *Renewable and Sustainable Energy Reviews*, *73*, 610-621. https://doi.org/https://doi.org/10.1016/j.rser.2017.01.166

Corona, A., Biddy, M. J., Vardon, D. R., Birkved, M., Hauschild, M. Z., & Beckham, G. T. (2018). Life cycle assessment of adipic acid production from lignin [10.1039/C8GC00868J]. *Green Chemistry*, *20*(16), 3857-3866. https://doi.org/10.1039/C8GC00868J

Elmore, J. R., Furches, A., Wolff, G. N., Gorday, K., & Guss, A. M. (2017). Development of a high efficiency integration system and promoter library for rapid modification of Pseudomonas putida KT2440. *Metab Eng Commun*, *5*, 1-8. https://doi.org/10.1016/j.meteno.2017.04.001

GIA. (2021). *Nylon - Global Market Trajectory & Analytics*. https://www.researchandmarkets.com/reports/1227800/nylon_global_market_trajectory_and_analytics?utm_source=BW&utm_medium=PressRelease&utm_code=zz65xc&utm_campaign=1419396+-+Global+Nylon+Market+Analysis+and+Outlook+2020-2027+-+Nylon+6+Volumes+Will+Reach+5.3+Million+Tons+by+2027%2c+Despite+COVID-19&utm_exec=joca220prd

Hartner, F. S., Ruth, C., Langenegger, D., Johnson, S. N., Hyka, P., Lin-Cereghino, G. P., Lin-Cereghino, J., Kovar, K., Cregg, J. M., & Glieder, A. (2008). Promoter library designed

for fine-tuned gene expression in Pichia pastoris. *Nucleic Acids Res*, *36*(12), e76. https://doi.org/10.1093/nar/gkn369
Hixson, J. L., & Ward, A. S. (2022). Hardware Selection and Performance of Low-Cost Fluorometers. *Sensors (Basel)*, *22*(6). https://doi.org/10.3390/s22062319
Hwang, H. J., Lee, S. Y., & Lee, P. C. (2018). Engineering and application of synthetic nar promoter for fine-tuning the expression of metabolic pathway genes in Escherichia coli. *Biotechnol Biofuels*, *11*, 103. https://doi.org/10.1186/s13068-018-1104-1
Inoue, H., Nojima, H., & Okayama, H. (1990). High efficiency transformation of Escherichia coli with plasmids. *Gene*, 23-28.
Ji, C. H., Kim, H., & Kang, H. S. (2019). Synthetic Inducible Regulatory Systems Optimized for the Modulation of Secondary Metabolite Production in Streptomyces. *ACS Synth Biol*, *8*(3), 577-586. https://doi.org/10.1021/acssynbio.9b00001
Klein, C. A., Teufel, M., Weile, C. J., & Sobetzko, P. (2021). The bacterial promoter spacer modulates promoter strength and timing by length, TG-motifs and DNA supercoiling sensitivity. *Sci Rep*, *11*(1), 24399. https://doi.org/10.1038/s41598-021-03817-4
Köbbing, S. (2020). Development of synthetic biology tools for Pseudomonas Putida. *Apprimus Verlag*, *23*.
Lee, S., Sohn, J.-H., Bae, J.-H., Kim, S. C., & Sung, B. H. (2020). Current Status of Pseudomonas putida Engineering for Lignin Valorization. *Biotechnology and Bioprocess Engineering*, *25*(6), 862-871. https://doi.org/10.1007/s12257-020-0029-2
Martínez-García, E., & de Lorenzo, V. (2012). Transposon-Based and Plasmid-Based Genetic Tools for Editing Genomes of Gram-Negative Bacteria. *W. Weber, & M. Fussenegger,* , *Synthetic Gene Networks: Methods and Protocols* 267-274.
Nguyen, L. T., Phan, D.-P., Sarwar, A., Tran, M. H., Lee, O. K., & Lee, E. Y. (2021). Valorization of industrial lignin to value-added chemicals by chemical depolymerization and biological conversion. *Industrial Crops and Products*, *161*, 113219. https://doi.org/https://doi.org/10.1016/j.indcrop.2020.113219
Nikel, P. I., & de Lorenzo, V. (2018). Pseudomonas putida as a functional chassis for industrial biocatalysis: From native biochemistry to trans-metabolism. *Metab Eng*, *50*, 142-155. https://doi.org/10.1016/j.ymben.2018.05.005
Nordholt, N., van Heerden, J., Kort, R., & Bruggeman, F. J. (2017). Effects of growth rate and promoter activity on single-cell protein expression. *Sci Rep*, *7*(1), 6299. https://doi.org/10.1038/s41598-017-05871-3
Pelley, J. W. (2012). 16 - RNA Transcription and Control of Gene Expression. In J. W. Pelley (Ed.), *Elsevier's Integrated Review Biochemistry (Second Edition)* (pp. 137-147). W.B. Saunders. https://doi.org/https://doi.org/10.1016/B978-0-323-07446-9.00016-7
Politi, N., Pasotti, L., Zucca, S., Casanova, M., Micoli, G., Cusella De Angelis, M. G., & Magni, P. (2014). Half-life measurements of chemical inducers for recombinant gene expression. *J Biol Eng*, *8*(1), 5. https://doi.org/10.1186/1754-1611-8-5
Ravi, K., Garcia-Hidalgo, J., Gorwa-Grauslund, M. F., & Liden, G. (2017). Conversion of lignin model compounds by Pseudomonas putida KT2440 and isolates from compost. *Appl Microbiol Biotechnol*, *101*(12), 5059-5070. https://doi.org/10.1007/s00253-017-8211-y
Ravi, K., García-Hidalgo, J., Nöbel, M., Gorwa-Grauslund, M. F., & Lidén, G. (2018). Biological conversion of aromatic monolignol compounds by a Pseudomonas isolate from sediments of the Baltic Sea. *AMB Express*, *8*(1), 1-14.
Salvachúa, D., Johnson, C. W., Singer, C. A., Rohrer, H., Peterson, D. J., Black, B. A., Knapp, A., & Beckham, G. T. (2018). Bioprocess development for muconic acid production from aromatic compounds and lignin. *Green Chemistry*, *20*(21), 5007-5019. https://doi.org/10.1039/c8gc02519c

Sathesh-Prabu, C., Tiwari, R., Kim, D., & Lee, S. K. (2021). Inducible and tunable gene expression systems for Pseudomonas putida KT2440. *Sci Rep*, *11*(1), 18079. https://doi.org/10.1038/s41598-021-97550-7

Wackett, L. P. (2003). Pseudomonas putida—a versatile biocatalyst. *Nature Biotechnology*, *21*(2), 136-138. https://doi.org/10.1038/nbt0203-136

Weimer, A., Kohlstedt, M., Volke, D. C., Nikel, P. I., & Wittmann, C. (2020). Industrial biotechnology of Pseudomonas putida: advances and prospects. *Appl Microbiol Biotechnol*, *104*(18), 7745-7766. https://doi.org/10.1007/s00253-020-10811-9

Wenger, J., Haas, V., & Stern, T. (2020). Why Can We Make Anything from Lignin Except Money? Towards a Broader Economic Perspective in Lignin Research. *Current Forestry Reports*, *6*(4), 294-308. https://doi.org/10.1007/s40725-020-00126-3

Wirth, N. T., & Nikel, P. I. (2021). Combinatorial pathway balancing provides biosynthetic access to 2-fluoro-cis,cis-muconate in engineered Pseudomonas putida. *Chem Catal*, *1*(6), 1234-1259. https://doi.org/10.1016/j.checat.2021.09.002

Zobel, S., Benedetti, I., Eisenbach, L., de Lorenzo, V., Wierckx, N., & Blank, L. M. (2015). Tn7-Based Device for Calibrated Heterologous Gene Expression in Pseudomonas putida. *ACS Synth Biol*, *4*(12), 1341-1351. https://doi.org/10.1021/acssynbio.5b00058

Appendix 1

Primer designs for PCR extension reactions.

Primer	Sequence	5’ overhang	5’ phosphorylation
msfGFP forward	5’-atgggcccgagctcagga-ggaaaaacatatgcgtaaaggtg-3’	ApaI-SacI	Yes
msfGFP reverse	5’aataagcttttatttgta-gagttcatccatgccgtg-3’	HindIII	Yes
p14c forward	5’-tttatgttgtataatataac-tactcacaccctaggccgcgg-3’	Promoter half	Yes
p14c reverse	5’-aattgacatgtcaattcact-tagactctcttccgggcgctatca-3’	Promoter half	Yes
p14g forward	5’-gcggccaggtataattgca-cgatcacaccctaggccgcgg-3’	Promoter half	Yes
p14g reverse	5’-gagagccttgtcaatgggc-gactctcttccgggcgctatca-3’	Promoter half	Yes

Primer designs for PCR verification.

Primer	Sequence
p14c forward	5’-gaattgacatgtcaatttttatgttg-3’
p14g forward	5’-gcccattgacaaggctctcg-3’
lacIq-Ptrc forward	5’-ccagtaacgttatacgatgtcgc-3’

msfGFP forward	5’-aggaggaaaaacatatgcgtaaaggtg-3’
msfGFP reverse	5’-ttatttgtagagttcatccatgccgtg-3’
p424 terminator	5’-ctggattctcaccaataaaaaacgc-3’

Promoter sequences.

Promoter	Sequence
p14c	5’-taagtgaattgacatgtcaatttttatgttgtataatataactac-3’
lacIq-Ptrc	5’- gtgaaaccagtaacgttatacgatgtcgcagagtatgccggtgtctcttatcagaccgtttcccgcgtggtgaaccaggccagccacgtttctgcgaaaacgcgggaaaaagtggaa gcggcgatggcggagctgaattacattcccaaccgcgtggcacaacaactggcgggcaaacagtcgttgctgattggcgttgccacctccagtctggccctgcacgcgccgtcgca aattgtcgcggcgattaaatctcgcgccgatcaactgggtgccagcgtggtggtgtcgatggtagaacgaagcggcgtcgaagcctgtaaagcggcggtgcacaatcttctcgcgc aacgcgtcagtgggctgatcattaactatccgctggatgaccaggatgccattgctgtggaagctgcctgcactaatgttccggcgttatttcttgatgtctctgaccagacacccatcaa cagtattatttttctcccatgaagacggtacgcgactgggcgtggagcatctggtcgcattgggtcaccagcaaatcgcgctgttagcgggcccattaagttctgtctcggcgcgtctgc gtctggctggctggcataaatatctcactcgcaatcaaattcagccgatagcggaacgggaaggcgactggagtgccatgtccggttttcaacaaaccatgcaaatgctgaatgagg gcatcgttcccactgcgatgctggttgccaacgatcagatggcgctgggcgcaatgcgcgccattaccgagtccgggctgcgcgttggtgcggatatctcggtagtgggatacgac gataccgaagacagctcatgttatatcccgccgttaaccaccatcaaacaggattttcgcctgctggggcaaaccagcgtggaccgcttgctgcaactctctcagggccaggcggtg aagggcaatcagctgttgcccgtctcactggtgaaaagaaaaaccaccctggcgcccaatacgcaaaccgcctctccccgcgcgttggccgattcattaatgcagctggcacgaca ggtttcccgactggaaagcgggcagtgagcgcaacgcaattaatgtaagttagcgcgaattgatctggtttgacagcttatcatcgactgcacggtgcaccaatgcttctggcgtcagg cagccatcggaagctgtggtatggctgtgcaggtcgtaaatcactgcataattcgtgtcgctcaaggcgcactcccgttctggataatgtttttgcgccgacatcataacggttctggca aatattctgaaatgagctgttgacaattaatcatccggctcgtataatg-3’
p14g	5’-gcccattgacaaggctctcgcggccaggtataattgcacga-3’
msfGFP	5’- atgcgtaaaggtgaagaactgttcaccggtgttgttccgatcctggttgaactggatggtgatgttaacggccacaaattctctgttcgtggtgaaggtgaaggtgatgcaaccaacggt aaactgaccctgaaattcatctgcactaccggtaaactgccggttccatggccgactctggtgactaccctgacctatggtgttcagtgtttttctcgttacccggatcacatgaagcagc atgatttcttcaaatctgcaatgccggaaggttatgtacaggagcgcaccatttctttcaaagacgatggcacctacaaaacccgtgcagaggttaaatttgaaggtgatactctggtgaa ccgtattgaactgaaaggcattgatttcaaagaggacggcaacatcctgggccacaaactggaatataacttcaactcccataacgtttacatcaccgcagacaaacagaagaacggt atcaaagctaacttcaaaattcgccataacgttgaagacggtagcgtacagctggcggaccactaccagcagaacactccgatcggtgatggtccggttctgctgccggataaccact acctgtccacccagtctaaactgtccaaagacccgaacgaaaagcgcgaccacatggtgctgctggagttcgttactgccgcaggtatcacgcacggcatggatgaactctacaaat aa-3’

Appendix 2

Growth curve of *P. putida* p427M in M9 media supplemented with different carbon sources.

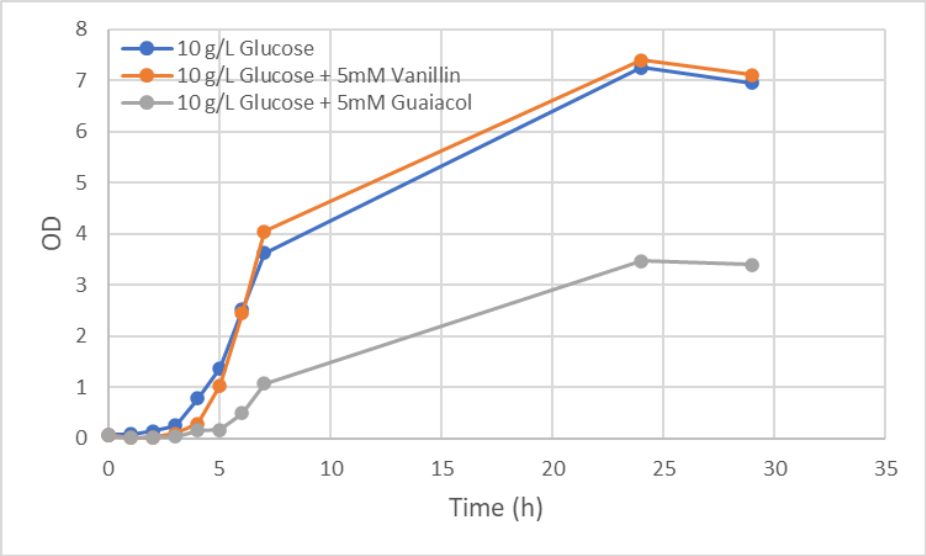

Appendix 3

Plasmid maps.

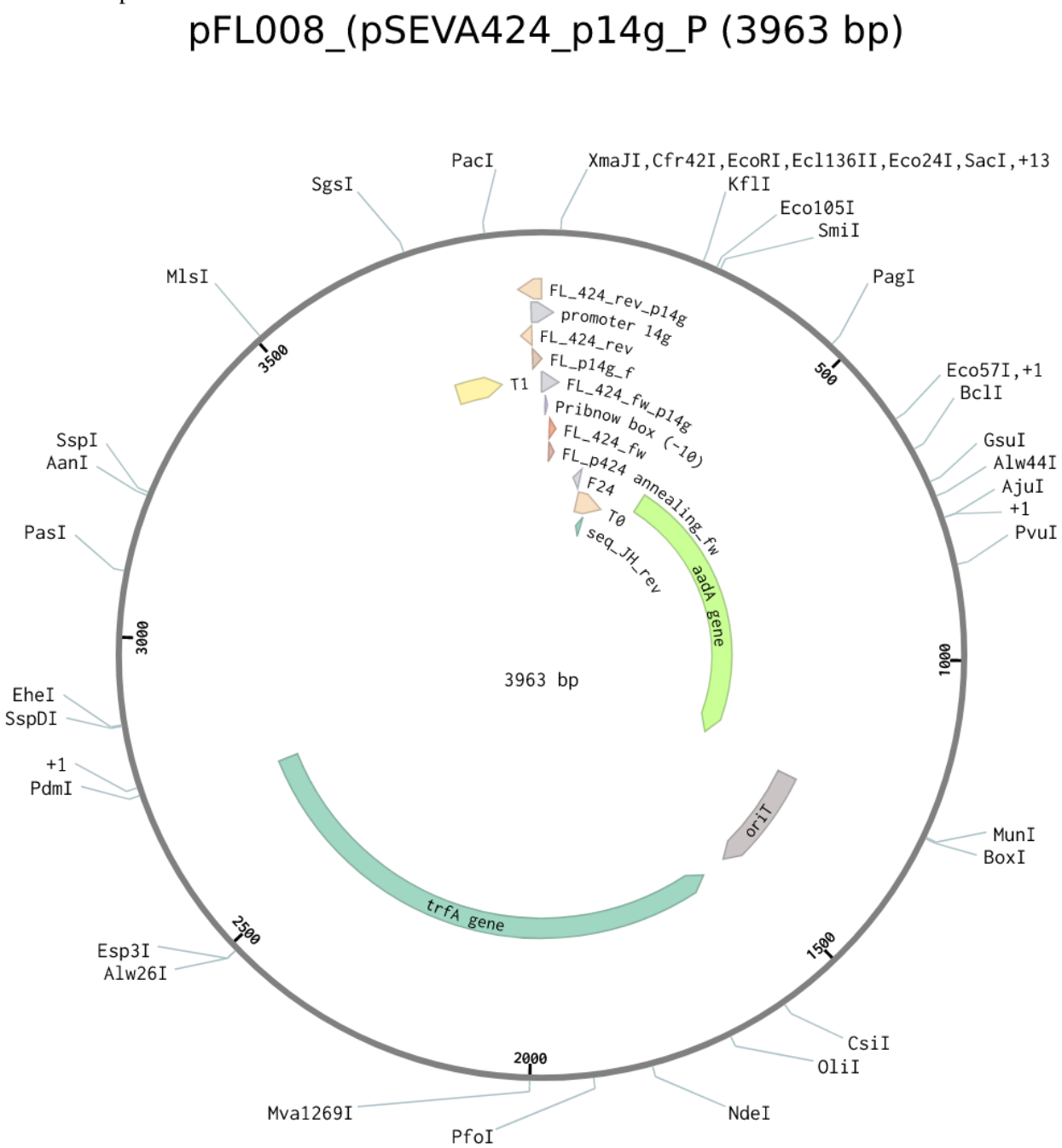

pFL010_(p14g,_msfgfp,_R (4655 bp)

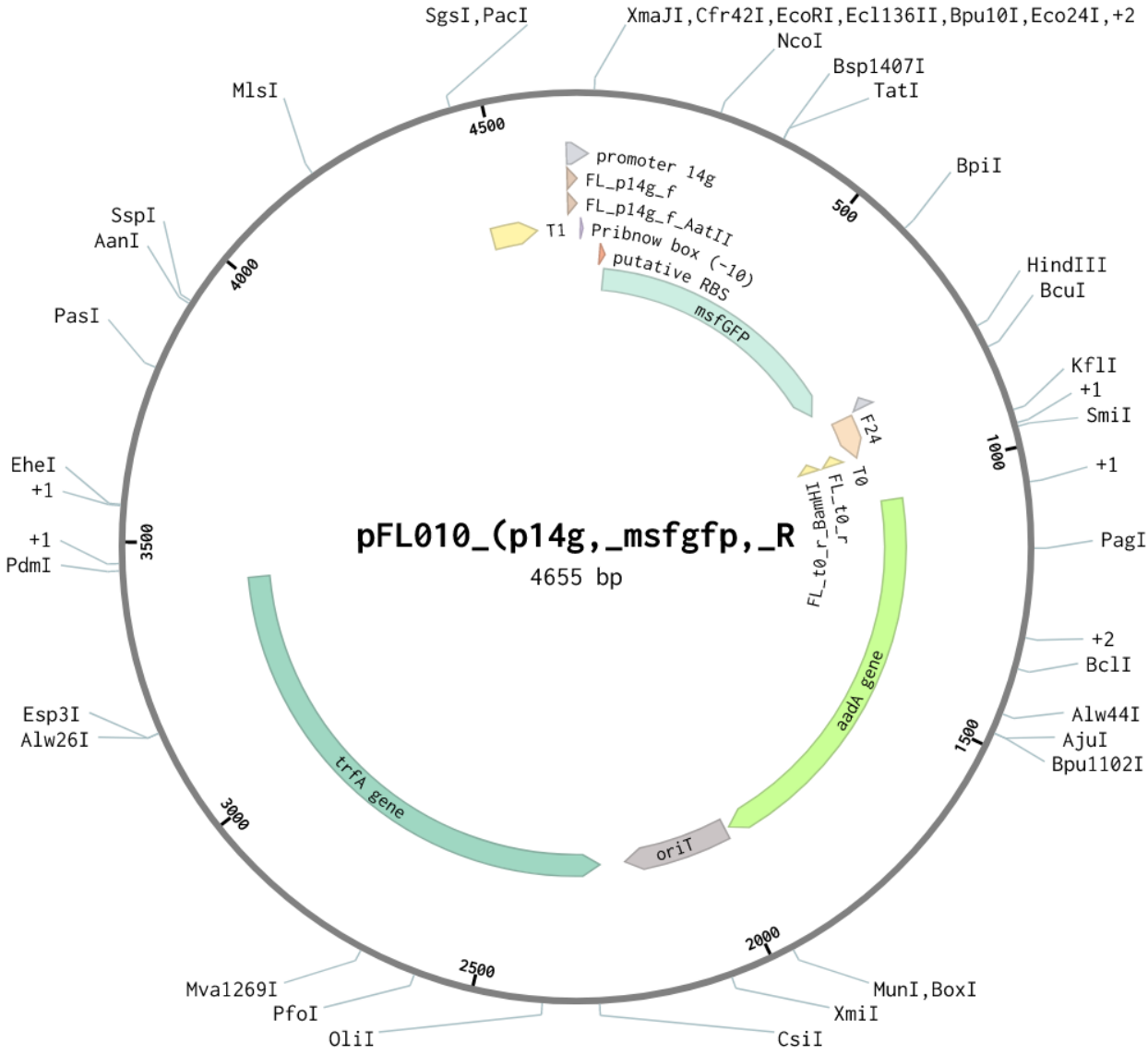

pFL013_pSEVA424_p14c_PC (3967 bp)

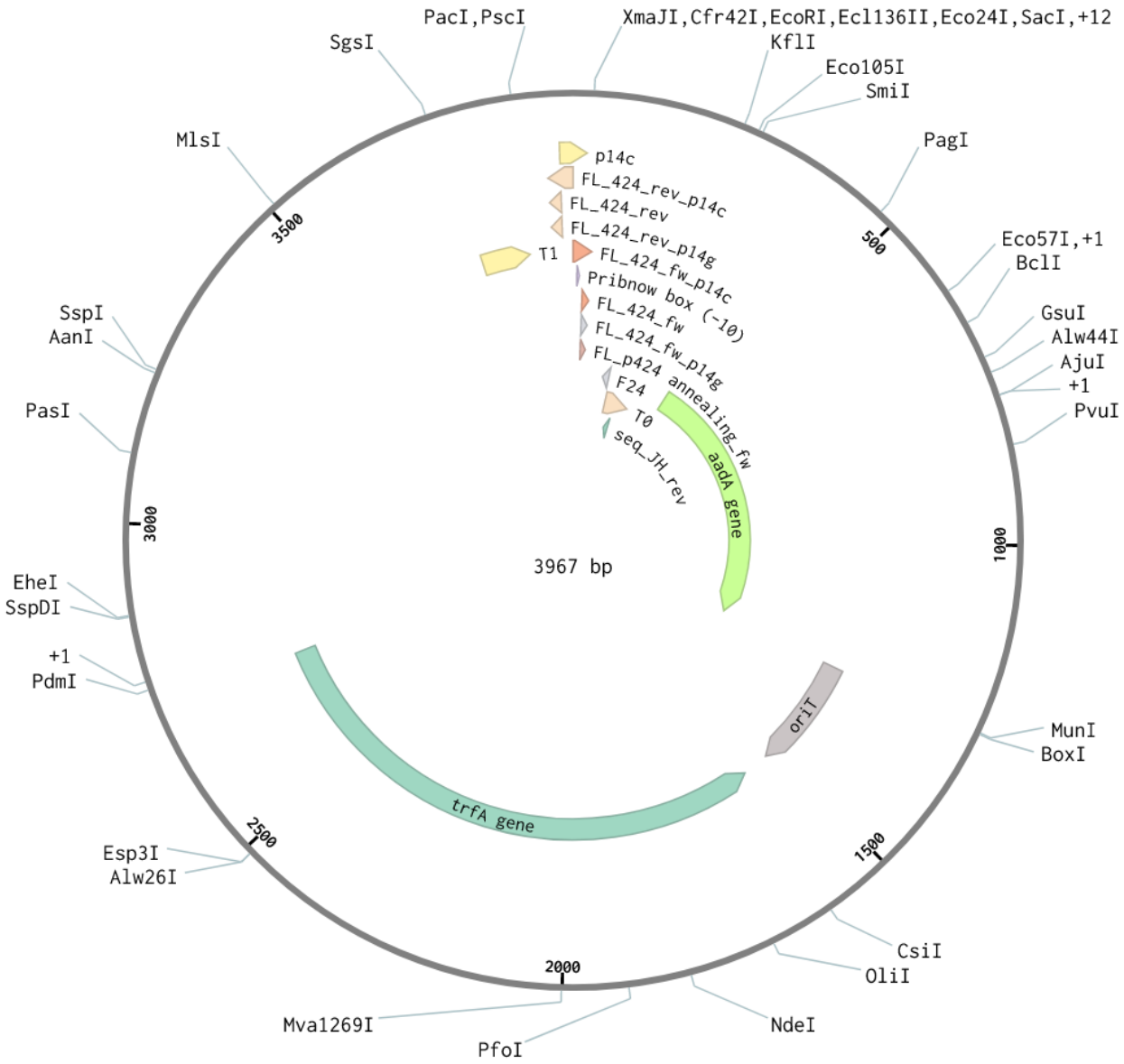

pFL014_p14c,_msfgfp (4659 bp)

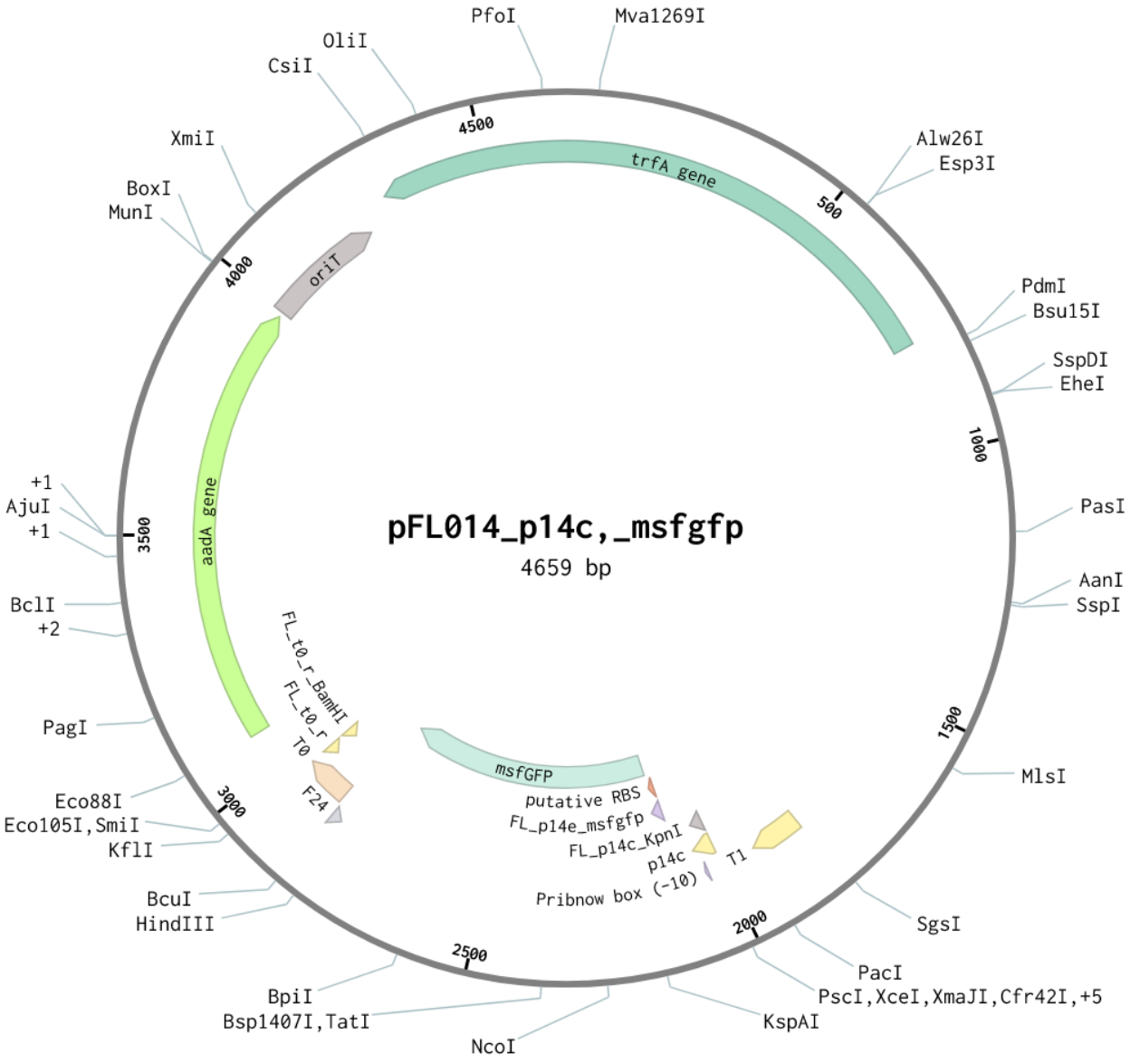

pFL015 (6001 bp)